The alloy concentration as a control parameter of the electron capture mechanism

2000 J. Phys.: Condens. Matter 12 10535

(http://iopscience.iop.org/0953-8984/12/50/314)

J. Phys.: Condens. Matter **12** (2000) 10535–10542. Printed in the UK PII: S0953-8984(00)15479-7

The alloy concentration as a control parameter of the electron capture mechanism

V N Stavrou

Physics Department, University of Essex, Colchester CO4 3SQ, UK
and
Theoretical Quantum Optic-Electronics, Institute of Technical Physics,
DLR Pfaffenwaldring 38–40, University of Stuttgart, D-70569 Stuttgart, Germany

E-mail: Vasilios.Stavrou@dlr.de

Received 14 July 2000, in final form 31 August 2000

Abstract. We present the electron capture rates for the double heterostructure GaAs/$Al_xGa_{1-x}As$ confined between two outer metallic barriers. The capture mechanism is assisted by the emission of bulk and dielectric continuum (DC) phonons. The alloys generate other phonon resonances compared with the electron capture rates, which are evaluated in the case of the GaAs/AlAs heterostructure. This investigation shows that the concentration of aluminium is an important parameter to control the electron capture mechanism.

1. Introduction

The alloys have a range of energy gaps depending on the concentration parameter x, which influences the phonon properties of the system and can be used for fabricating blue–green semiconductor lasers. The alloy system $Al_xGa_{1-x}As$ is mainly important for fabricating high speed electronic and optoelectronic devices because the lattice mismatch with GaAs is very small [1]. An important factor for describing quantum well laser emission is the electron capture rates. Several research groups [2–8] have studied the capture mechanism using different approaches.

There are two different physical situations which can be realized in a semiconductor heterostructure with different parameters. The first (and the physically more straightforward situation) is when the electron energy spectrum is quantized (discrete) in both the barrier and quantum well regions [4]. In essence this coincides with the practical case of a 'quantum well inside a quantum well' laser system. The physical requirement for the realization of this situation is that the electron coherence length be of the order of or larger than the entire structure width. The simplest way to estimate the electron coherence length is to equate it to the electron mean free path. In this case the electron can propagate without scattering and without loss of phase. As a result, a standing-wave-like state can be established; the quantum mechanical consequence of this is that the probability flux density $\boldsymbol{J} = (i\hbar/2m^*)[\Psi^*\nabla\Psi - (\nabla\Psi^*)\Psi]$ is zero, so that the electron does not carry any momentum. The energy spectrum is therefore discrete, with the states inside and outside the quantum well obtainable by solving Schrödinger's equation, and is determined by the size of the smaller quantum well as well as the width of the entire structure. The capture process in this case should be considered in terms of inter-subband transitions between discrete states. Clearly the magnitude of the capture rates

0953-8984/00/5010535+08$30.00

will then depend on the entire size of the structure. The capture rate, evaluated by Fermi's golden rule, is an appropriate parameter. This situation has been experimentally studied by Blom *et al* [8], where the total size of the structure was about 1000 Å.

The second physical situation corresponds to the case where the width of the barrier region is large relative to the mean free path [5]. In this case the motion of the electron between external barriers is not coherent due to scattering, which results in the loss of electron phase. A standing-wave-like state cannot thus be established. In essence this is a bulk-like state which belongs to the quasi-continuous electron energy spectrum that does not depend on the size of the entire structure. However, since the width of the inner quantum well is typically much smaller than a mean free path, the electron motion through the quantum well region is ballistic. This means that the electron wave will undergo quantum mechanical processes (e.g. reflection and transmission) due to the quantum well potential. Thus the wavefunction in the continuum spectrum deviates from the simple plane wave solution. In contrast to the first case above, the quantum mechanical consequence of the present case is that the probability flux is non-zero (i.e. the electron carries a momentum). The capture process in this case should be considered in terms of transitions between continuous (unlocalized) and discrete (localized) states. Again the capture process is described by Fermi's golden rule, but the only parameter that is appropriate for the description of the capture process in this case is not the capture rates, but the capture velocity which ensures that there is no dependence on the entire structure size. However, all the characteristics of the inner quantum well are retained in the capture velocity.

In our investigation we will use the first method that has been described above. Concerning the heterostructures made with alloys, in order to investigate the effects of changing of the alloy concentration, we have evaluated the electron capture rates for the double heterostructure $GaAs/Al_xGa_{1-x}As$ quantum well. This evaluation shows that the concentration of the alloys could be used as control parameter for the electron capture rates.

2. Electron states and phonon modes

We consider the quantum well heterostructure $GaAs/Al_xGa_{1-x}As$ with well width $2L$ which is confined between metallic barriers. The metallic barriers will generate a discrete energy spectrum with energies larger than the depth of the well. Taking into account the continuity of the wavefunctions at the interfaces, the vanishing of the wavefunctions at the outer interfaces $z = -D$, D and finally the continuity of $1/m_i^*(\partial\Psi/\partial z)$ (where m_i^* is the effective mass in material i ($i = 1, 2$)) at the interfaces, gives rise to the following equations:

$$\Psi_s(\boldsymbol{r}, z) = A_s \exp(\mathrm{i}\boldsymbol{k}_\parallel \cdot \boldsymbol{r}) \begin{cases} \sinh[k_2(D-L)]\cos(k_1 z) & |z| \leqslant L \\ \cos(k_1 L)\sinh[k_2(D-|z|)] & L \leqslant |z| \leqslant D \end{cases} \tag{1}$$

$$\Psi_a(\boldsymbol{r}, z) = A_a \exp(\mathrm{i}\boldsymbol{k}_\parallel \cdot \boldsymbol{r}) \begin{cases} \sinh[k_2(D-L)]\sin(k_1 z) & |z| \leqslant L \\ \mathrm{sgn}(z)\sin(k_1 L)\sinh[k_2(D-|z|)] & L \leqslant |z| \leqslant D \end{cases} \tag{2}$$

where $\boldsymbol{r} = (\boldsymbol{r}_\parallel, z)$ is the position vector and $\boldsymbol{k}_\parallel$ is a two dimensional wavevector along the interface planes and $\mathrm{sgn}(z)$ is the sign of z. The coefficients A_s, A_a are defined by normalization of symmetric and antisymmetric wavefunctions respectively.

By using the boundary conditions, the symmetric and antisymmetric electron dispersion relations are given respectively by:

$$m_1^* k_2 \cos(k_1 L)\cosh[k_2(D-L)] - m_2^* k_1 \sin(k_1 L)\sinh[k_2(D-L)] = 0 \tag{3}$$

$$m_1^* k_2 \sin(k_1 L)\cosh[k_2(D-L)] + m_2^* k_1 \cos(k_1 L)\sinh[k_2(D-L)] = 0 \tag{4}$$

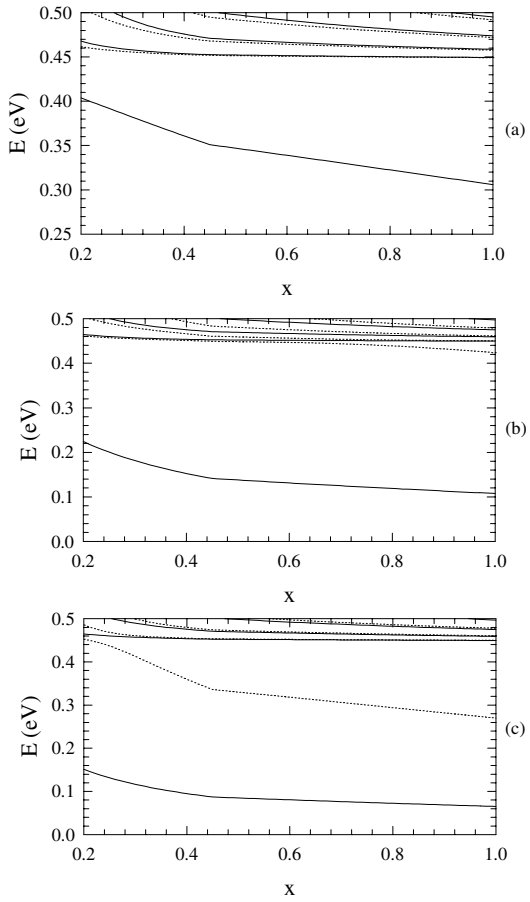

Figure 1. The energy levels for the quantum well GaAs/$Al_xGa_{1-x}As$ with half the well width (a) $L = 5.6$ Å, (b) $L = 20$ Å and (c) $L = 30$ Å and fixed total width $D = 300$ Å against the aluminium concentration parameter x. Solid lines are the symmetric and dotted lines are the antisymmetric energy levels.

where m_1^* and m_2^* are the electron effective masses for GaAs and $Al_xGa_{1-x}As$ respectively. The total energy of the electron is given by, $E_n(k_\parallel) = E_n + \hbar^2 k_\parallel^2/2m_1^*$, $E_n = \hbar^2 k_1^2/2m_1^*$ (assuming that the subbands are parabolic) and the wavevector in the barrier region is given by $k_2 = \sqrt{2m_2^* V_0/\hbar^2 - m_2^* k_1^2/m_1^*}$. The value of k_2 is real when $E_n < V_0$; otherwise it is imaginary.

Figure 1 shows the energy levels versus the concentration x for the heterostructure GaAs/$Al_xGa_{1-x}As$ for several well widths (the values for the material parameters are mentioned in [1]). It is seen that the bound states have smaller energies with increasing concentration of the alloy. For high values of alloy concentration the electron states do not enter the well (the electron energy is larger than the depth of the well). This observation, as we will see later, is important for the capture rates when designing alloys that are suitable for emission in the desired region of the electromagnetic spectrum.

In this investigation the scattering mechanism is assisted by bulk and DC phonons which are described by [9] and [10]. For the bulk phonon there is only one mode with a frequency

corresponding to the LO phonon of the bulk material and the DC consists of two kinds of mode, confined (Conf.) and interface modes (IP). For bulk phonons the second-quantized interaction Hamiltonian is given by

$$\hat{H}_I^B(\boldsymbol{r}, z, t) = \sum_j \int [C_B(\boldsymbol{q}) \exp[\mathrm{i}(\boldsymbol{q}_\parallel \cdot \boldsymbol{r} + q_z z - \omega t)]\hat{a}_q + HC]\, \mathrm{d}^3 q. \tag{5}$$

$\hat{a}_q(\hat{a}_q^\dagger)$ is the annihilation (creation) operator satisfying the usual commutator relationships for a bulk phonon with wavevector $\boldsymbol{q} = (\boldsymbol{q}_\parallel, q_z)$, HC stands for Hermitian conjugate and

$$C_B(\boldsymbol{q}) = -\frac{\mathrm{i}}{4q}\left[\frac{\mathrm{e}^2\hbar\omega_{L1}}{\pi^3\varepsilon_0}\left(\frac{1}{\varepsilon_{\infty 1}} - \frac{1}{\varepsilon_{s1}}\right)\right]^{1/2} \tag{6}$$

where ε_0 is the permittivity of free space, $\varepsilon_{\infty 1}$ and ε_{s1} are the high-frequency dielectric constant and the static dielectric constant for the GaAs respectively.

For the confined modes the interaction Hamiltonian is given by

$$\hat{H}_I(\boldsymbol{r}, z, t) = \begin{cases} \displaystyle\sum_j \int \left[C_{Conf2}(j, \boldsymbol{q}_\parallel, z) \exp[\mathrm{i}(\boldsymbol{q}_\parallel \cdot \boldsymbol{r} - \omega t)]\hat{a}_{j,\boldsymbol{q}_\parallel} + HC\right] \mathrm{d}^2 q_\parallel \\ \qquad\qquad -D \leqslant z \leqslant -L \\ \displaystyle\sum_m \int \left[C_{Conf1}(m, \boldsymbol{q}_\parallel, z) \exp[\mathrm{i}(\boldsymbol{q}_\parallel \cdot \boldsymbol{r} - \omega t)]\hat{a}_{m,\boldsymbol{q}_\parallel} + HC\right] \mathrm{d}^2 q_\parallel \\ \qquad\qquad |z| \leqslant L \\ \displaystyle\sum_n \int \left[C_{Conf2}(n, \boldsymbol{q}_\parallel, z) \exp[\mathrm{i}(\boldsymbol{q}_\parallel \cdot \boldsymbol{r} - \omega t)]\hat{a}_{n,\boldsymbol{q}_\parallel} + HC\right] \mathrm{d}^2 q_\parallel \\ \qquad\qquad L \leqslant z \leqslant D. \end{cases} \tag{7}$$

The confined modes have zero potential at the interfaces and have a frequency corresponding to the LO phonon of the material.

Lastly, the interaction Hamiltonian for interface modes is given by

$$\hat{H}_I^{IP}(\boldsymbol{r}, z, t) = \sum_{j,m} \int \left[C_{IP}^j(m, \boldsymbol{q}_\parallel, z) \exp[\mathrm{i}(\boldsymbol{q}_\parallel \cdot \boldsymbol{r} - \omega t)]\hat{a}_{m,\boldsymbol{q}_\parallel} + HC\right] \mathrm{d}^2 q_\parallel \tag{8}$$

where j denotes the symmetry and m specifies the IP mode. The boundary conditions for the IP modes, except for the continuity at the inner interfaces, have to vanish at the outer interfaces. In equations (7) and (8), the coefficients are calculated by using the boundary conditions mentioned above [4].

The dielectric functions for GaAs and $\mathrm{Al}_x\mathrm{Ga}_{1-x}\mathrm{As}$, which have a two-mode behaviour [1], are given by:

$$\varepsilon_1(\omega) = \varepsilon_{\infty 1}\frac{\omega^2 - \omega_{L1}^2}{\omega^2 - \omega_{T1}^2} \qquad \varepsilon_2(\omega) = \varepsilon_{\infty 2}\frac{\omega^2 - \omega_{L2,Ga}^2}{\omega^2 - \omega_{T2,Ga}^2}\frac{\omega^2 - \omega_{L2,Al}^2}{\omega^2 - \omega_{T2,Al}^2} \tag{9}$$

where the labels Ga and Al denote the GaAs-like and AlAs-like frequencies. The values for the zone centre LO, TO frequencies and the high frequency dielectric constants depend on the aluminium concentration x [1]. Thus the number of interface modes (IP) and the confined modes which comprise the DC model increases due to GaAs-like and AlAs-like frequencies. The IP modes consist of three symmetric and three antisymmetric modes [1]. The dispersion relations of the symmetric and antisymmetric IP modes are given respectively by

$$\frac{\varepsilon_1(\omega)}{\varepsilon_2(\omega)} = -\coth(q_\parallel(D - L))\coth(q_\parallel L) \tag{10}$$

$$\frac{\varepsilon_1(\omega)}{\varepsilon_2(\omega)} = -\coth(q_\parallel(D - L))\tanh(q_\parallel L) \tag{11}$$

which are found by the requirements of the boundary conditions.

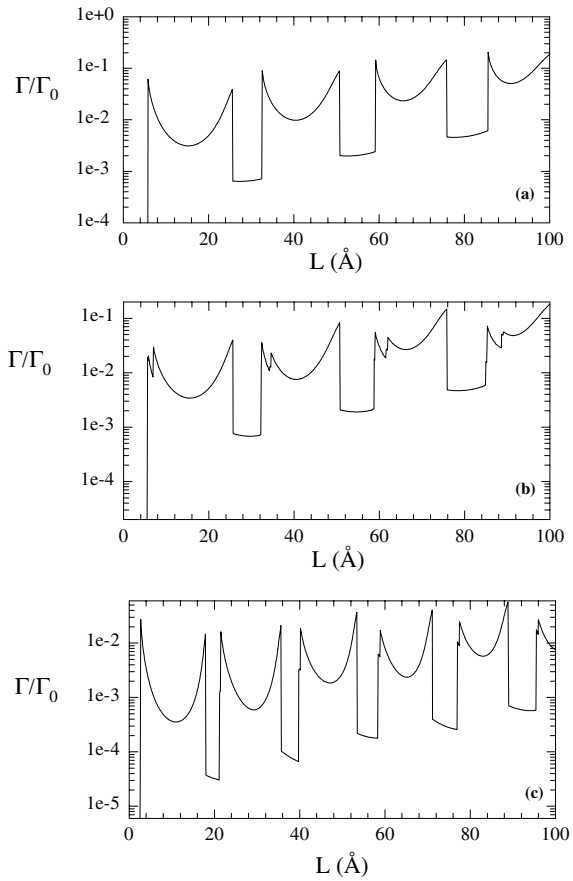

Figure 2. Variation with half the width L. (a) The electron capture rates (normalized to Γ_0) by the emission of bulk phonons, (b) DC phonons for the heterostructure GaAs/$Al_xGa_{1-x}As$ and (c) DC phonon for the heterostructure GaAs/AlAs quantum well with $D = 300$ Å and $x = 0.3$.

3. Capture rates

The capture rates have been defined as the transition rates of electrons from the bottom of the first subband (i) above the well to all possible states within subbands in the quantum well (n). The capture rates are given by Fermi's golden rule as

$$\Gamma = \frac{2\pi}{\hbar} \sum_{\text{all modes}} \sum_{\text{all final states } n} |\langle \Psi_n\{\boldsymbol{q}_\parallel\}|\hat{H}_I|\Psi_i\{0\}\rangle|^2 \delta\left(\frac{\hbar^2 q_\parallel^2}{2m_1^*} + \hbar\omega_{q_\parallel} - \Delta E_{i,n}\right) \tag{12}$$

where $\{\boldsymbol{q}_\parallel\}$ represents a single bulk or DC phonon state of wavevector $\boldsymbol{q}_\parallel$ and $\{0\}$ the vacuum state. It is convenient to present capture rates in terms of the characteristic rate Γ_0 for bulk GaAs which is given by

$$\Gamma_0 = \frac{e^2}{4\pi\varepsilon_0\hbar}\left(\frac{1}{\varepsilon_{\infty 1}} - \frac{1}{\varepsilon_{s1}}\right)\left(\frac{2m_1^*\omega_{L1}}{\hbar}\right)^{1/2}$$

which has a value of approximately 8.7×10^{12} s^{-1}.

The capture rates by emission of bulk phonons are given by equation (12). In figure 2(a) we show the variation of the electron capture rates against half the well width L for the

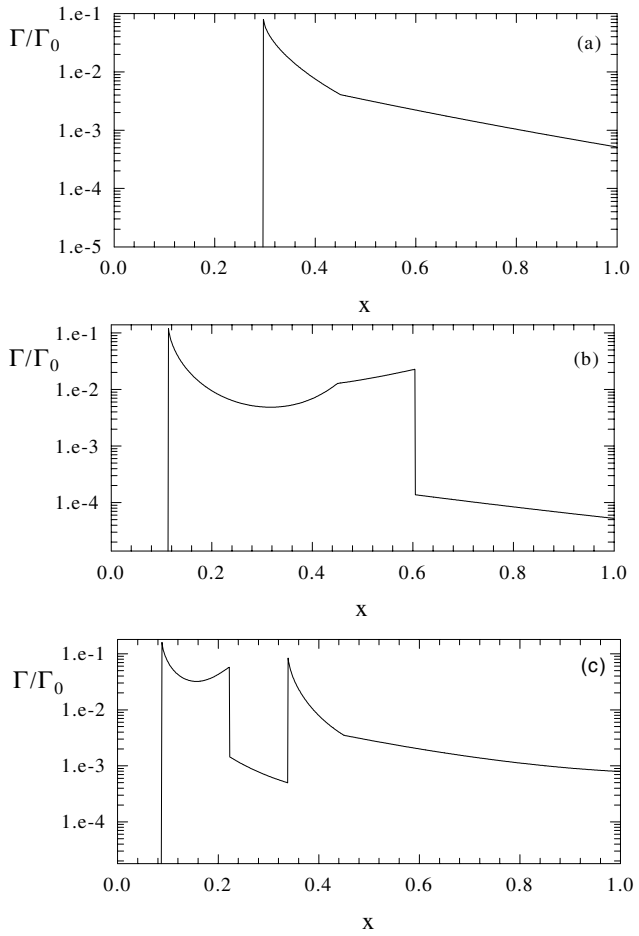

Figure 3. The electron capture rates by the emission of bulk phonons for the double heterostructure GaAs/Al_xGa_{1-x}As quantum well with total width $D = 300$ Å versus the concentration x for fixed half-well width (a) $L = 5.8$ Å (b) $L = 20$ Å and (c) $L = 30$ Å.

double heterostructure GaAs/Al_xGa_{1-x}As quantum well, which is assisted by the bulk phonon emission. In figure 2(b) we present the capture rates by the emission of DC phonons versus half the well width for the GaAs/Al_xGa_{1-x}As structure. The electron resonances appear when the electron states enter the well. Then the probability distribution for the electrons shifts from the barrier regions to the well and increases the overlap integrals in the matrix elements. The phonon resonances appear when the energy differences between the initial and the final state are equal to a phonon energy. In the case of the alloy system, extra phonon resonances appear because the dielectric function for Al_xGa_{1-x}As has a two-mode behaviour and so there are more phonon resonances. The capture rates for GaAs/AlAs are illustrated in figure 2(c), in which is clear that in the case of the GaAs/Al_xGa_{1-x}As structure extra phonon resonances appear because there are more modes that contribute to the transition mechanism. Furthermore, in the case of the heterostructure GaAs/AlAs, more regular intervals emerge where phonon–electron resonances exist due to the fact that the effective masses and energy gaps are different for different aluminium concentrations.

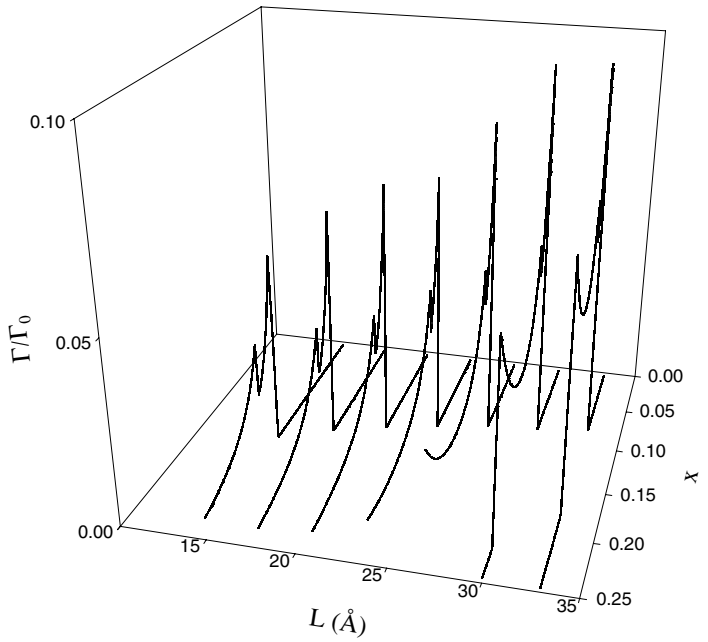

Figure 4. The electron capture rates by the emission of DC phonons for the heterostructure GaAs/$Al_xGa_{1-x}As$ with $D = 300$ Å versus half the well width L and aluminium concentration x.

The variation of capture rates with the concentration parameter x for the case of nitride alloys or II–VI systems can be exploited to predict which concentration is suitable to generate quantum well laser structures operating in the blue–green region of the electromagnetic spectrum or for shorter wavelengths [11]. The capture rates, versus the concentration of the alloys for the GaAs/$Al_xGa_{1-x}As$ system by the emission of bulk phonons, are shown in figure 3. For $L = 5.8$ Å and $x = 0.3$ the first phonon resonance occurs, as seen in figure 2(a). In figure 3(a) for $x = 0.3$ a phonon resonance appears and the capture rates decrease subsequently because the number of energy levels (figure 1) decreases with increasing alloy concentration. There is no electron resonance because for the half well width $L = 5.8$ Å (figure 1) the electron states no longer enter the well and, as a result, the wavefunctions concentrate in the barrier regions. Therefore the overlap in the matrix element does not become large and so the capture rates decrease with increasing alloy concentration. It is only by increasing the fixed value of well width that the number of electron states increases and more electron states enter the well with increasing concentration. This is the reason why in figures 3(b) and (c) there is an electron resonance. After the electron resonance there is no phonon resonance (figure 3(b)) because the electron states no longer enter the well and the phonon wavevector becomes large with increasing concentration. As a result, there is no phonon resonance and the capture rates decrease with x. In figure 3(c) a new phonon resonance appears due to the fact that the energy difference between the initial and final state becomes equal to the LO energy. By increasing the concentration the capture rates decrease because the energy difference becomes large.

The combined effects of the variations of the alloy concentration and the well width on the capture rates are presented in figure 4. The electron resonances appear when the electron states enter the quantum well and the phonon resonances when the energy difference is equal to the LO energy. As can be seen, the electron and phonon resonances shift with increasing alloy

concentration. Therefore by fixing the well and barrier widths and changing the concentration the transition rates vary between small and resonance values.

4. Conclusions

In our investigation, we have taken into account only the electron–phonon interactions and we have neglected effects such as the temperature effects, relaxation rates, recombination of the electrons and the alloy scattering itself. It has been reported that the electron capture velocities strongly depend on the temperature for different heterostructures (GaN/AlN, GaAs/AlAs) [5]. The aim of this work is the investigation of electron capture by the emission of LO phonons and the dependence of the capture rates on alloy concentration and neglects any other effect.

Summing overall, the electron capture rates for QWs made with alloys by the emission of bulk and DC phonons are in a very good agreement (figures 2(a), (b)). The electron resonances have the same magnitudes but the phonon resonances occur in different well widths and have different magnitudes due to the fact that bulk and DC phonons have different frequencies. On the other hand the number of phonon resonances is larger than the case of GaAs/AlAs due to the two-mode behaviour of alloys. Lastly, the numerical evaluation shows that by fixing the well and barrier widths and changing the concentration, the transition rates vary between small values and resonance values. Thus, the alloy concentration could be an important parameter to control the electron capture mechanism. This observation could be useful for experiments dealing with the electron capture process for studies of semiconductor lasers that could operate in the desired regime of wavelengths. According to the best of the author's knowledge, such experiments have not been reported in order to compare them with our theoretical results.

Acknowledgments

The author would like to thank Professor B K Ridley and Dr C R Bennett for many interesting and fruitful discussions about the results of this work.

References

[1] Adachi S 1985 *J. Appl. Phys.* **58** R1
[2] Brum J A and Bastard G 1986 *Phys. Rev.* B **33** 1420
[3] Kozyrev S V and Shik Ya A 1985 *Sov. Phys.–Semicond.* **19** 1025
[4] Stavrou V N, Bennett C R, Babiker M, Zakhleniuk N A and Ridley B K 1998 *Phys. Low-Dim. Struct.* **1/2** 23
[5] Zakhleniuk N A, Bennett C R, Stavrou V N, Babiker M, and Ridley B K 1999 *Phys. Status Solidi* a **176** 79
Zakleniuk N A, Ridley B K, Babiker M and Bennett C R 1998 *Proc. ICPS 24 (Jerusalem)* (Singapore: World Scientific)
[6] Yassievich N, Schmalz K and Beer M 1994 *Semicond. Sci. Technol.* **9** 1763
[7] Mansour N S, Kim K W and Littlejohn M A 1995 *J. Appl. Phys.* **77** 2834
[8] Blom P W, Smith C, Haverkort J E M and Wolter J H 1993 *Phys. Rev.* B **47** 2072
[9] Fuchs R and Kliewer K L 1965 *Phys. Rev.* A **140** 2076
Kliewer K L and Fuchs R 1966 *Phys. Rev.* **144** 495
[10] Mori N and Ando T 1989 *Phys. Rev.* B **40** 6175
[11] Fasol G and Nakamura S 1997 *The Blue Laser Diode GaN Based Light Emitters and Lasers* (Berlin: Springer)